# Measurement of the $\bar{B}\_s^0 \to D\_s^- D\_s^+$ and $\bar{B}\_s^0 \to D^- D\_s^+$ effective lifetimes

R. Aaij, Y. Amhis, S. Barsuk, O. Callot, J. He, O. Kochebina, J. Lefrançois,
F. Machefert, A. Martin Sanchez, M. Nicol, et al.

## HAL Id: in2p3-00914272
## https://hal.in2p3.fr/in2p3-00914272

Submitted on 21 Sep 2023

EUROPEAN ORGANIZATION FOR NUCLEAR RESEARCH (CERN)

# Measurement of the $\overline{B}_s^0 \to D_s^- D_s^+$ and $\overline{B}_s^0 \to D^- D_s^+$ effective lifetimes

The LHCb collaboration[†]

**Abstract**

The first measurement of the effective lifetime of the $\overline{B}_s^0$ meson in the decay $\overline{B}_s^0 \to D_s^- D_s^+$ is reported using a proton-proton collision dataset, corresponding to an integrated luminosity of $3\,\mathrm{fb}^{-1}$, collected by the LHCb experiment. The measured value of the $\overline{B}_s^0 \to D_s^- D_s^+$ effective lifetime is $1.379 \pm 0.026 \pm 0.017$ ps, where the uncertainties are statistical and systematic, respectively. This lifetime translates into a measurement of the decay width of the light $\overline{B}_s^0$ mass eigenstate of $\Gamma_{\mathrm{L}} = 0.725 \pm 0.014 \pm 0.009\ \mathrm{ps}^{-1}$. The $\overline{B}_s^0$ lifetime is also measured using the flavor-specific $\overline{B}_s^0 \to D^- D_s^+$ decay to be $1.52 \pm 0.15 \pm 0.01$ ps.

[†]Authors are listed on the following pages.

# LHCb collaboration

R. Aaij[40], B. Adeva[36], M. Adinolfi[45], A. Affolder[51], Z. Ajaltouni[5], J. Albrecht[9], F. Alessio[37], M. Alexander[50], S. Ali[40], G. Alkhazov[29], P. Alvarez Cartelle[36], A.A. Alves Jr[24], S. Amato[2], S. Amerio[21], Y. Amhis[7], L. Anderlini[17,g], J. Anderson[39], R. Andreassen[56], M. Andreotti[16,f], J.E. Andrews[57], R.B. Appleby[53], O. Aquines Gutierrez[10], F. Archilli[37], A. Artamonov[34], M. Artuso[58], E. Aslanides[6], G. Auriemma[24,n], M. Baalouch[5], S. Bachmann[11], J.J. Back[47], A. Badalov[35], V. Balagura[30], W. Baldini[16], R.J. Barlow[53], C. Barschel[38], S. Barsuk[7], W. Barter[46], V. Batozskaya[27], Th. Bauer[40], A. Bay[38], J. Beddow[50], F. Bedeschi[22], I. Bediaga[1], S. Belogurov[30], K. Belous[34], I. Belyaev[30], E. Ben-Haim[8], G. Bencivenni[18], S. Benson[49], J. Benton[45], A. Berezhnoy[31], R. Bernet[39], M.-O. Bettler[46], M. van Beuzekom[40], A. Bien[11], S. Bifani[44], T. Bird[53], A. Bizzeti[17,i], P.M. Bjørnstad[53], T. Blake[47], F. Blanc[38], J. Blouw[10], S. Blusk[58], V. Bocci[24], A. Bondar[33], N. Bondar[29], W. Bonivento[15,37], S. Borghi[53], A. Borgia[58], M. Borsato[7], T.J.V. Bowcock[51], E. Bowen[39], C. Bozzi[16], T. Brambach[9], J. van den Brand[41], J. Bressieux[38], D. Brett[53], M. Britsch[10], T. Britton[58], N.H. Brook[45], H. Brown[51], A. Bursche[39], G. Busetto[21,r], J. Buytaert[37], S. Cadeddu[15], R. Calabrese[16,f], O. Callot[7], M. Calvi[20,k], M. Calvo Gomez[35,p], A. Camboni[35], P. Campana[18,37], D. Campora Perez[37], A. Carbone[14,d], G. Carboni[23,l], R. Cardinale[19,j], A. Cardini[15], H. Carranza-Mejia[49], L. Carson[49], K. Carvalho Akiba[2], G. Casse[51], L. Castillo Garcia[37], M. Cattaneo[37], Ch. Cauet[9], R. Cenci[57], M. Charles[8], Ph. Charpentier[37], S.-F. Cheung[54], N. Chiapolini[39], M. Chrzaszcz[39,25], K. Ciba[37], X. Cid Vidal[37], G. Ciezarek[52], P.E.L. Clarke[49], M. Clemencic[37], H.V. Cliff[46], J. Closier[37], C. Coca[28], V. Coco[37], J. Cogan[6], E. Cogneras[5], P. Collins[37], A. Comerma-Montells[35], A. Contu[15,37], A. Cook[45], M. Coombes[45], S. Coquereau[8], G. Corti[37], B. Couturier[37], G.A. Cowan[49], D.C. Craik[47], M. Cruz Torres[59], S. Cunliffe[52], R. Currie[49], C. D'Ambrosio[37], J. Dalseno[45], P. David[8], P.N.Y. David[40], A. Davis[56], I. De Bonis[4], K. De Bruyn[40], S. De Capua[53], M. De Cian[11], J.M. De Miranda[1], L. De Paula[2], W. De Silva[56], P. De Simone[18], D. Decamp[4], M. Deckenhoff[9], L. Del Buono[8], N. Déléage[4], D. Derkach[54], O. Deschamps[5], F. Dettori[41], A. Di Canto[11], H. Dijkstra[37], S. Donleavy[51], F. Dordei[11], P. Dorosz[25,o], A. Dosil Suárez[36], D. Dossett[47], A. Dovbnya[42], F. Dupertuis[38], P. Durante[37], R. Dzhelyadin[34], A. Dziurda[25], A. Dzyuba[29], S. Easo[48], U. Egede[52], V. Egorychev[30], S. Eidelman[33], D. van Eijk[40], S. Eisenhardt[49], U. Eitschberger[9], R. Ekelhof[9], L. Eklund[50,37], I. El Rifai[5], Ch. Elsasser[39], A. Falabella[16,f], C. Färber[11], C. Farinelli[40], S. Farry[51], D. Ferguson[49], V. Fernandez Albor[36], F. Ferreira Rodrigues[1], M. Ferro-Luzzi[37], S. Filippov[32], M. Fiore[16,f], M. Fiorini[16,f], C. Fitzpatrick[37], M. Fontana[10], F. Fontanelli[19,j], R. Forty[37], O. Francisco[2], M. Frank[37], C. Frei[37], M. Frosini[17,37,g], E. Furfaro[23,l], A. Gallas Torreira[36], D. Galli[14,d], M. Gandelman[2], P. Gandini[58], Y. Gao[3], J. Garofoli[58], P. Garosi[53], J. Garra Tico[46], L. Garrido[35], C. Gaspar[37], R. Gauld[54], E. Gersabeck[11], M. Gersabeck[53], T. Gershon[47], Ph. Ghez[4], A. Gianelle[21], V. Gibson[46], L. Giubega[28], V.V. Gligorov[37], C. Göbel[59], D. Golubkov[30], A. Golutvin[52,30,37], A. Gomes[1,a], H. Gordon[37], M. Grabalosa Gándara[5], R. Graciani Diaz[35], L.A. Granado Cardoso[37], E. Graugés[35], G. Graziani[17], A. Grecu[28], E. Greening[54], S. Gregson[46], P. Griffith[44], L. Grillo[11], O. Grünberg[60], B. Gui[58], E. Gushchin[32], Yu. Guz[34,37], T. Gys[37], C. Hadjivasiliou[58], G. Haefeli[38], C. Haen[37], T.W. Hafkenscheid[62], S.C. Haines[46], S. Hall[52], B. Hamilton[57], T. Hampson[45], S. Hansmann-Menzemer[11], N. Harnew[54], S.T. Harnew[45], J. Harrison[53], T. Hartmann[60], J. He[37], T. Head[37], V. Heijne[40], K. Hennessy[51], P. Henrard[5], J.A. Hernando Morata[36], E. van Herwijnen[37], M. Heß[60], A. Hicheur[1], D. Hill[54], M. Hoballah[5],

C. Hombach[53], W. Hulsbergen[40], P. Hunt[54], T. Huse[51], N. Hussain[54], D. Hutchcroft[51], D. Hynds[50], V. Iakovenko[43], M. Idzik[26], P. Ilten[55], R. Jacobsson[37], A. Jaeger[11], E. Jans[40], P. Jaton[38], A. Jawahery[57], F. Jing[3], M. John[54], D. Johnson[54], C.R. Jones[46], C. Joram[37], B. Jost[37], N. Jurik[58], M. Kaballo[9], S. Kandybei[42], W. Kanso[6], M. Karacson[37], T.M. Karbach[37], I.R. Kenyon[44], T. Ketel[41], B. Khanji[20], S. Klaver[53], O. Kochebina[7], I. Komarov[38], R.F. Koopman[41], P. Koppenburg[40], M. Korolev[31], A. Kozlinskiy[40], L. Kravchuk[32], K. Kreplin[11], M. Kreps[47], G. Krocker[11], P. Krokovny[33], F. Kruse[9], M. Kucharczyk[20,25,37,k], V. Kudryavtsev[33], K. Kurek[27], T. Kvaratskheliya[30,37], V.N. La Thi[38], D. Lacarrere[37], G. Lafferty[53], A. Lai[15], D. Lambert[49], R.W. Lambert[41], E. Lanciotti[37], G. Lanfranchi[18], C. Langenbruch[37], T. Latham[47], C. Lazzeroni[44], R. Le Gac[6], J. van Leerdam[40], J.-P. Lees[4], R. Lefèvre[5], A. Leflat[31], J. Lefrançois[7], S. Leo[22], O. Leroy[6], T. Lesiak[25], B. Leverington[11], Y. Li[3], M. Liles[51], R. Lindner[37], C. Linn[11], F. Lionetto[39], B. Liu[3], G. Liu[37], S. Lohn[37], I. Longstaff[50], J.H. Lopes[2], N. Lopez-March[38], P. Lowdon[39], H. Lu[3], D. Lucchesi[21,r], J. Luisier[38], H. Luo[49], E. Luppi[16,f], O. Lupton[54], F. Machefert[7], I.V. Machikhiliyan[30], F. Maciuc[28], O. Maev[29,37], S. Malde[54], G. Manca[15,e], G. Mancinelli[6], J. Maratas[5], U. Marconi[14], P. Marino[22,t], R. Märki[38], J. Marks[11], G. Martellotti[24], A. Martens[8], A. Martín Sánchez[7], M. Martinelli[40], D. Martinez Santos[41], D. Martins Tostes[2], A. Martynov[31], A. Massafferri[1], R. Matev[37], Z. Mathe[37], C. Matteuzzi[20], A. Mazurov[16,37,f], M. McCann[52], J. McCarthy[44], A. McNab[53], R. McNulty[12], B. McSkelly[51], B. Meadows[56,54], F. Meier[9], M. Meissner[11], M. Merk[40], D.A. Milanes[8], M.-N. Minard[4], J. Molina Rodriguez[59], S. Monteil[5], D. Moran[53], M. Morandin[21], P. Morawski[25], A. Mordà[6], M.J. Morello[22,t], R. Mountain[58], I. Mous[40], F. Muheim[49], K. Müller[39], R. Muresan[28], B. Muryn[26], B. Muster[38], P. Naik[45], T. Nakada[38], R. Nandakumar[48], I. Nasteva[1], M. Needham[49], S. Neubert[37], N. Neufeld[37], A.D. Nguyen[38], T.D. Nguyen[38], C. Nguyen-Mau[38,q], M. Nicol[7], V. Niess[5], R. Niet[9], N. Nikitin[31], T. Nikodem[11], A. Novoselov[34], A. Oblakowska-Mucha[26], V. Obraztsov[34], S. Oggero[40], S. Ogilvy[50], O. Okhrimenko[43], R. Oldeman[15,e], G. Onderwater[62], M. Orlandea[28], J.M. Otalora Goicochea[2], P. Owen[52], A. Oyanguren[35], B.K. Pal[58], A. Palano[13,c], M. Palutan[18], J. Panman[37], A. Papanestis[48,37], M. Pappagallo[50], L. Pappalardo[16], C. Parkes[53], C.J. Parkinson[9], G. Passaleva[17], G.D. Patel[51], M. Patel[52], C. Patrignani[19,j], C. Pavel-Nicorescu[28], A. Pazos Alvarez[36], A. Pearce[53], A. Pellegrino[40], G. Penso[24,m], M. Pepe Altarelli[37], S. Perazzini[14,d], E. Perez Trigo[36], P. Perret[5], M. Perrin-Terrin[6], L. Pescatore[44], E. Pesen[63], G. Pessina[20], K. Petridis[52], A. Petrolini[19,j], E. Picatoste Olloqui[35], B. Pietrzyk[4], T. Pilař[47], D. Pinci[24], S. Playfer[49], M. Plo Casasus[36], F. Polci[8], G. Polok[25], A. Poluektov[47,33], E. Polycarpo[2], A. Popov[34], D. Popov[10], B. Popovici[28], C. Potterat[35], A. Powell[54], J. Prisciandaro[38], A. Pritchard[51], C. Prouve[45], V. Pugatch[43], A. Puig Navarro[38], G. Punzi[22,s], W. Qian[4], B. Rachwal[25], J.H. Rademacker[45], B. Rakotomiaramanana[38], M. Rama[18], M.S. Rangel[2], I. Raniuk[42], N. Rauschmayr[37], G. Raven[41], S. Redford[54], S. Reichert[53], M.M. Reid[47], A.C. dos Reis[1], S. Ricciardi[48], A. Richards[52], K. Rinnert[51], V. Rives Molina[35], D.A. Roa Romero[5], P. Robbe[7], D.A. Roberts[57], A.B. Rodrigues[1], E. Rodrigues[53], P. Rodriguez Perez[36], S. Roiser[37], V. Romanovsky[34], A. Romero Vidal[36], M. Rotondo[21], J. Rouvinet[38], T. Ruf[37], F. Ruffini[22], H. Ruiz[35], P. Ruiz Valls[35], G. Sabatino[24,l], J.J. Saborido Silva[36], N. Sagidova[29], P. Sail[50], B. Saitta[15,e], V. Salustino Guimaraes[2], B. Sanmartin Sedes[36], R. Santacesaria[24], C. Santamarina Rios[36], E. Santovetti[23,l], M. Sapunov[6], A. Sarti[18], C. Satriano[24,n], A. Satta[23], M. Savrie[16,f], D. Savrina[30,31], M. Schiller[41], H. Schindler[37], M. Schlupp[9], M. Schmelling[10], B. Schmidt[37], O. Schneider[38], A. Schopper[37], M.-H. Schune[7], R. Schwemmer[37], B. Sciascia[18],

iv

A. Sciubba[24], M. Seco[36], A. Semennikov[30], K. Senderowska[26], I. Sepp[52], N. Serra[39],
J. Serrano[6], P. Seyfert[11], M. Shapkin[34], I. Shapoval[16,42,f], Y. Shcheglov[29], T. Shears[51],
L. Shekhtman[33], O. Shevchenko[42], V. Shevchenko[61], A. Shires[9], R. Silva Coutinho[47],
G. Simi[21], M. Sirendi[46], N. Skidmore[45], T. Skwarnicki[58], N.A. Smith[51], E. Smith[54,48],
E. Smith[52], J. Smith[46], M. Smith[53], H. Snoek[40], M.D. Sokoloff[56], F.J.P. Soler[50], F. Soomro[38],
D. Souza[45], B. Souza De Paula[2], B. Spaan[9], A. Sparkes[49], P. Spradlin[50], F. Stagni[37],
S. Stahl[11], O. Steinkamp[39], S. Stevenson[54], S. Stoica[28], S. Stone[58], B. Storaci[39], S. Stracka[22,37],
M. Straticiuc[28], U. Straumann[39], R. Stroili[21], V.K. Subbiah[37], L. Sun[56], W. Sutcliffe[52],
S. Swientek[9], V. Syropoulos[41], M. Szczekowski[27], P. Szczypka[38,37], D. Szilard[2], T. Szumlak[26],
S. T'Jampens[4], M. Teklishyn[7], G. Tellarini[16,f], E. Teodorescu[28], F. Teubert[37], C. Thomas[54],
E. Thomas[37], J. van Tilburg[11], V. Tisserand[4], M. Tobin[38], S. Tolk[41], L. Tomassetti[16,f],
D. Tonelli[37], S. Topp-Joergensen[54], N. Torr[54], E. Tournefier[4,52], S. Tourneur[38], M.T. Tran[38],
M. Tresch[39], A. Tsaregorodtsev[6], P. Tsopelas[40], N. Tuning[40], M. Ubeda Garcia[37], A. Ukleja[27],
A. Ustyuzhanin[61], U. Uwer[11], V. Vagnoni[14], G. Valenti[14], A. Vallier[7], R. Vazquez Gomez[18],
P. Vazquez Regueiro[36], C. Vázquez Sierra[36], S. Vecchi[16], J.J. Velthuis[45], M. Veltri[17,h],
G. Veneziano[38], M. Vesterinen[11], B. Viaud[7], D. Vieira[2], X. Vilasis-Cardona[35,p], A. Vollhardt[39],
D. Volyanskyy[10], D. Voong[45], A. Vorobyev[29], V. Vorobyev[33], C. Voß[60], H. Voss[10],
J.A. de Vries[40], R. Waldi[60], C. Wallace[47], R. Wallace[12], S. Wandernoth[11], J. Wang[58],
D.R. Ward[46], N. Warrington[58], N.K. Watson[44], A.D. Webber[53], D. Websdale[52],
M. Whitehead[47], J. Wicht[37], J. Wiechczynski[25], D. Wiedner[11], L. Wiggers[40], G. Wilkinson[54],
M.P. Williams[47,48], M. Williams[55], F.F. Wilson[48], J. Wimberley[57], J. Wishahi[9], W. Wislicki[27],
M. Witek[25], G. Wormser[7], S.A. Wotton[46], S. Wright[46], S. Wu[3], K. Wyllie[37], Y. Xie[49,37],
Z. Xing[58], Z. Yang[3], X. Yuan[3], O. Yushchenko[34], M. Zangoli[14], M. Zavertyaev[10,b], F. Zhang[3],
L. Zhang[58], W.C. Zhang[12], Y. Zhang[3], A. Zhelezov[11], A. Zhokhov[30], L. Zhong[3], A. Zvyagin[37].

[1]*Centro Brasileiro de Pesquisas Físicas (CBPF), Rio de Janeiro, Brazil*
[2]*Universidade Federal do Rio de Janeiro (UFRJ), Rio de Janeiro, Brazil*
[3]*Center for High Energy Physics, Tsinghua University, Beijing, China*
[4]*LAPP, Université de Savoie, CNRS/IN2P3, Annecy-Le-Vieux, France*
[5]*Clermont Université, Université Blaise Pascal, CNRS/IN2P3, LPC, Clermont-Ferrand, France*
[6]*CPPM, Aix-Marseille Université, CNRS/IN2P3, Marseille, France*
[7]*LAL, Université Paris-Sud, CNRS/IN2P3, Orsay, France*
[8]*LPNHE, Université Pierre et Marie Curie, Université Paris Diderot, CNRS/IN2P3, Paris, France*
[9]*Fakultät Physik, Technische Universität Dortmund, Dortmund, Germany*
[10]*Max-Planck-Institut für Kernphysik (MPIK), Heidelberg, Germany*
[11]*Physikalisches Institut, Ruprecht-Karls-Universität Heidelberg, Heidelberg, Germany*
[12]*School of Physics, University College Dublin, Dublin, Ireland*
[13]*Sezione INFN di Bari, Bari, Italy*
[14]*Sezione INFN di Bologna, Bologna, Italy*
[15]*Sezione INFN di Cagliari, Cagliari, Italy*
[16]*Sezione INFN di Ferrara, Ferrara, Italy*
[17]*Sezione INFN di Firenze, Firenze, Italy*
[18]*Laboratori Nazionali dell'INFN di Frascati, Frascati, Italy*
[19]*Sezione INFN di Genova, Genova, Italy*
[20]*Sezione INFN di Milano Bicocca, Milano, Italy*
[21]*Sezione INFN di Padova, Padova, Italy*
[22]*Sezione INFN di Pisa, Pisa, Italy*
[23]*Sezione INFN di Roma Tor Vergata, Roma, Italy*
[24]*Sezione INFN di Roma La Sapienza, Roma, Italy*

[25] *Henryk Niewodniczanski Institute of Nuclear Physics Polish Academy of Sciences, Kraków, Poland*

[26] *AGH - University of Science and Technology, Faculty of Physics and Applied Computer Science, Kraków, Poland*

[27] *National Center for Nuclear Research (NCBJ), Warsaw, Poland*

[28] *Horia Hulubei National Institute of Physics and Nuclear Engineering, Bucharest-Magurele, Romania*

[29] *Petersburg Nuclear Physics Institute (PNPI), Gatchina, Russia*

[30] *Institute of Theoretical and Experimental Physics (ITEP), Moscow, Russia*

[31] *Institute of Nuclear Physics, Moscow State University (SINP MSU), Moscow, Russia*

[32] *Institute for Nuclear Research of the Russian Academy of Sciences (INR RAN), Moscow, Russia*

[33] *Budker Institute of Nuclear Physics (SB RAS) and Novosibirsk State University, Novosibirsk, Russia*

[34] *Institute for High Energy Physics (IHEP), Protvino, Russia*

[35] *Universitat de Barcelona, Barcelona, Spain*

[36] *Universidad de Santiago de Compostela, Santiago de Compostela, Spain*

[37] *European Organization for Nuclear Research (CERN), Geneva, Switzerland*

[38] *Ecole Polytechnique Fédérale de Lausanne (EPFL), Lausanne, Switzerland*

[39] *Physik-Institut, Universität Zürich, Zürich, Switzerland*

[40] *Nikhef National Institute for Subatomic Physics, Amsterdam, The Netherlands*

[41] *Nikhef National Institute for Subatomic Physics and VU University Amsterdam, Amsterdam, The Netherlands*

[42] *NSC Kharkiv Institute of Physics and Technology (NSC KIPT), Kharkiv, Ukraine*

[43] *Institute for Nuclear Research of the National Academy of Sciences (KINR), Kyiv, Ukraine*

[44] *University of Birmingham, Birmingham, United Kingdom*

[45] *H.H. Wills Physics Laboratory, University of Bristol, Bristol, United Kingdom*

[46] *Cavendish Laboratory, University of Cambridge, Cambridge, United Kingdom*

[47] *Department of Physics, University of Warwick, Coventry, United Kingdom*

[48] *STFC Rutherford Appleton Laboratory, Didcot, United Kingdom*

[49] *School of Physics and Astronomy, University of Edinburgh, Edinburgh, United Kingdom*

[50] *School of Physics and Astronomy, University of Glasgow, Glasgow, United Kingdom*

[51] *Oliver Lodge Laboratory, University of Liverpool, Liverpool, United Kingdom*

[52] *Imperial College London, London, United Kingdom*

[53] *School of Physics and Astronomy, University of Manchester, Manchester, United Kingdom*

[54] *Department of Physics, University of Oxford, Oxford, United Kingdom*

[55] *Massachusetts Institute of Technology, Cambridge, MA, United States*

[56] *University of Cincinnati, Cincinnati, OH, United States*

[57] *University of Maryland, College Park, MD, United States*

[58] *Syracuse University, Syracuse, NY, United States*

[59] *Pontifícia Universidade Católica do Rio de Janeiro (PUC-Rio), Rio de Janeiro, Brazil, associated to [2]*

[60] *Institut für Physik, Universität Rostock, Rostock, Germany, associated to [11]*

[61] *National Research Centre Kurchatov Institute, Moscow, Russia, associated to [30]*

[62] *KVI - University of Groningen, Groningen, The Netherlands, associated to [40]*

[63] *Celal Bayar University, Manisa, Turkey, associated to [37]*

[a] *Universidade Federal do Triângulo Mineiro (UFTM), Uberaba-MG, Brazil*

[b] *P.N. Lebedev Physical Institute, Russian Academy of Science (LPI RAS), Moscow, Russia*

[c] *Università di Bari, Bari, Italy*

[d] *Università di Bologna, Bologna, Italy*

[e] *Università di Cagliari, Cagliari, Italy*

[f] *Università di Ferrara, Ferrara, Italy*

[g] *Università di Firenze, Firenze, Italy*

[h] *Università di Urbino, Urbino, Italy*

[i] *Università di Modena e Reggio Emilia, Modena, Italy*

[j] *Università di Genova, Genova, Italy*

$^{k}$*Università di Milano Bicocca, Milano, Italy*

$^{l}$*Università di Roma Tor Vergata, Roma, Italy*

$^{m}$*Università di Roma La Sapienza, Roma, Italy*

$^{n}$*Università della Basilicata, Potenza, Italy*

$^{o}$*AGH - University of Science and Technology, Faculty of Computer Science, Electronics and Telecommunications, Kraków, Poland*

$^{p}$*LIFAELS, La Salle, Universitat Ramon Llull, Barcelona, Spain*

$^{q}$*Hanoi University of Science, Hanoi, Viet Nam*

$^{r}$*Università di Padova, Padova, Italy*

$^{s}$*Università di Pisa, Pisa, Italy*

$^{t}$*Scuola Normale Superiore, Pisa, Italy*

A central goal in quark-flavor physics is to test whether the Cabibbo-Kobayashi-Maskawa (CKM) mechanism [1,2] can fully describe all relevant weak decay observables, or if physics beyond the Standard Model (SM) is needed. In the neutral $B$ meson sector, the mass eigenstates do not coincide with the flavor eigenstates as a result of $B\bar{B}$ mixing. In addition to measurable mass splittings between the mass eigenstates [3], the $B_s$ system also exhibits a sizeable difference in the decay widths $\Gamma_\mathrm{L}$ and $\Gamma_\mathrm{H}$, where the subscripts L and H refer to the light and heavy mass eigenstates, respectively. This difference is due to the large decay width to final states accessible to both $B_s^0$ and $\bar{B}_s^0$. In the absence of $CP$ violation, the mass eigenstates are also eigenstates of $CP$. The summed decay rate of $B_s^0$ and $\bar{B}_s^0$ to the $CP$-even $D_s^+D_s^-$ final state can be written as [4]

$$\Gamma_{\bar{B}_s^0 \to D_s^- D_s^+}(t) + \Gamma_{B_s^0 \to D_s^+ D_s^-}(t) \propto (1 + \cos\phi_s)e^{-\Gamma_\mathrm{L}t} + (1 - \cos\phi_s)e^{-\Gamma_\mathrm{H}t}, \qquad (1)$$

where $\phi_s$ is the ($CP$-violating) relative weak phase between the $\bar{B}_s^0$ mixing and $b \to c\bar{c}s$ decay amplitudes.

The untagged decay rate in Eq. 1 provides a probe of $\phi_s$, $\Gamma_\mathrm{L}$ and $\Gamma_\mathrm{H}$ in a way that is complementary to direct determinations using $CP$ violating asymmetries [5]. Approximating Eq. 1 by a single exponential

$$\Gamma_{\bar{B}_s^0 \to D_s^- D_s^+}(t) + \Gamma_{B_s^0 \to D_s^+ D_s^-}(t) \propto e^{-t/\tau_{\bar{B}_s^0 \to D_s^- D_s^+}^{\mathrm{eff}}}, \qquad (2)$$

defines the $\bar{B}_s^0 \to D_s^- D_s^+$ effective lifetime, which can be written as $\tau_{\bar{B}_s^0 \to D_s^- D_s^+}^{\mathrm{eff}} = \tau_{\bar{B}_s^0}(1 - y_s\cos\phi_s + \mathcal{O}(y_s^2))$ [4,6], assuming no direct $CP$ violation in the $\bar{B}_s^0 \to D_s^- D_s^+$ decay. Here $y_s \equiv \Delta\Gamma_s/(2\Gamma_s)$, $\Delta\Gamma_s \equiv \Gamma_\mathrm{L} - \Gamma_\mathrm{H}$ and $\Gamma_s = (\Gamma_\mathrm{H} + \Gamma_\mathrm{L})/2 = 1/\tau_{\bar{B}_s^0}$, where $\tau_{\bar{B}_s^0}$ is the flavor-specific $\bar{B}_s^0$ lifetime. Using the measured value of $\phi_s = 0.01 \pm 0.07 \pm 0.01$ rad [5], which is in good agreement with the SM expectation of $-0.0363^{+0.0016}_{-0.0015}$ rad [7], it follows that $\tau_{\bar{B}_s^0 \to D_s^- D_s^+}^{\mathrm{eff}} \simeq \Gamma_\mathrm{L}^{-1}$.

The most precise measurement to date of the effective lifetime in a $CP$-even final state used $\bar{B}_s^0 \to K^+K^-$ [8] decays, and yielded a value $\tau_{\bar{B}_s^0 \to K^+K^-}^{\mathrm{eff}} = 1.455 \pm 0.046\,(\mathrm{stat}) \pm 0.006\,(\mathrm{syst})$ ps. Loop contributions, both within, and possibly beyond the SM, are expected to be significantly larger in $\bar{B}_s^0 \to K^+K^-$ than in $\bar{B}_s^0 \to D_s^- D_s^+$. These contributions give rise to direct $CP$ violation in the $\bar{B}_s^0 \to K^+K^-$ decay [9], which lead to differences between $\tau^{\mathrm{eff}}$ in these two $CP$ final state decays, making a comparison of their effective lifetimes interesting. Measurements have also been made in $CP$-odd modes, such as $\bar{B}_s^0 \to J/\psi\, f_0(980)$ [10,11] and $\bar{B}_s^0 \to J/\psi\, K_\mathrm{S}^0$ [12]. The most precise value is from the former, yielding $\tau_{\bar{B}_s^0 \to J/\psi\, f_0(980)}^{\mathrm{eff}} = 1.700 \pm 0.040\,(\mathrm{stat}) \pm 0.026\,(\mathrm{syst})$ ps [10]. Constraints from these measurements on the $(\Delta\Gamma_s,\ \phi_s)$ parameter space are given in Refs. [4,13]. Improved precision on the effective lifetimes will enable more stringent tests of the consistency between the direct measurements of $\Delta\Gamma_s$ and $\phi_s$, and those inferred using effective lifetimes.

In this Letter, the $\bar{B}_s^0 \to D_s^- D_s^+$ time-dependent decay rate is normalized to the corresponding rate in the $B^- \to D^0 D_s^-$ decay, which has similar final state topology and kinematic properties, and a precisely measured lifetime of $\tau_{B^-} = 1.641 \pm 0.008$ ps [14]. As

a result, many of the systematic uncertainties cancel in the measured ratio. The relative rate is then given by

$$\frac{\Gamma_{\bar{B}_s^0 \to D_s^- D_s^+}(t) + \Gamma_{B_s^0 \to D_s^+ D_s^-}(t)}{\Gamma_{B^- \to D^0 D_s^-}(t) + \Gamma_{B^+ \to \bar{D}^0 D_s^+}(t)} \propto e^{-\alpha_{su} t}, \tag{3}$$

where $\alpha_{su} = 1/\tau_{\bar{B}_s^0 \to D_s^- D_s^+}^{\text{eff}} - 1/\tau_{B^-}$. A measurement of $\alpha_{su}$ therefore determines $\tau_{\bar{B}_s^0 \to D_s^- D_s^+}^{\text{eff}}$.

The $\bar{B}_s^0$ meson lifetime is also measured using the flavor-specific, Cabibbo-suppressed $\bar{B}_s^0 \to D^- D_s^+$ decay. Its time-dependent rate is normalized to that of the $B^0 \to D^- D_s^+$ decay. In what follows, the symbol $B$ without a flavor designation refers to either a $B^-$, $\bar{B}^0$ or $\bar{B}_s^0$ meson, and $D$ refers to either a $D^0$, $D^+$ or $D_s^+$ meson. Unless otherwise indicated, charge conjugate final states are included.

The measurements presented use a proton-proton ($pp$) collision data sample corresponding to 3 fb$^{-1}$ of integrated luminosity, 1 fb$^{-1}$ recorded at a center-of-mass energy of 7 TeV and 2 fb$^{-1}$ at 8 TeV, collected by the LHCb experiment. The LHCb detector [15] is a single-arm forward spectrometer covering the pseudorapidity range $2 < \eta < 5$, designed for the study of particles containing $b$ or $c$ quarks. The detector includes a high-precision tracking system consisting of a silicon-strip vertex detector surrounding the $pp$ interaction region, a large-area silicon-strip detector located upstream of a dipole magnet with a bending power of about 4 Tm, and three stations of silicon-strip detectors and straw drift tubes placed downstream. The combined tracking system provides a momentum measurement with relative uncertainty that varies from 0.4% at 5 GeV/$c$ to 0.6% at 100 GeV/$c$, and impact parameter (IP) resolution of 20 μm for tracks with large transverse momentum ($p_{\text{T}}$). Ring-imaging Cherenkov detectors [16] are used to distinguish charged hadrons, and photon, electron and hadron candidates are identified by a calorimeter system consisting of scintillating-pad and preshower detectors, an electromagnetic calorimeter and a hadronic calorimeter. Muons are identified by a system composed of alternating layers of iron and multiwire proportional chambers [17].

The trigger [18] consists of a hardware stage, based on information from the calorimeter and muon systems, followed by a software stage, which applies a full event reconstruction [18, 19]. No specific requirement is made on the hardware trigger decision. Of the $B$ meson candidates considered in this analysis, about 60% are triggered at the hardware level by one or more of the final state particles in the signal $B$ decay. The remaining 40% are triggered due to other activity in the event. The software trigger requires a two-, three- or four-track secondary vertex with a large sum of the transverse momentum of the tracks and a significant displacement from the primary $pp$ interaction vertices (PVs). At least one track should have $p_{\text{T}} > 1.7$ GeV/$c$ and $\chi_{\text{IP}}^2$ with respect to any primary interaction greater than 16, where $\chi_{\text{IP}}^2$ is defined as the difference in $\chi^2$ of a given PV reconstructed with and without the considered particle included. The signal candidates used in this analysis are required to pass a multivariate software trigger selection algorithm [19].

Proton-proton collisions are simulated using Pythia [20] with a specific LHCb configuration [21]. Decays of hadronic particles are described by EvtGen [22], in which final state radiation is generated using Photos [23]. The interaction of the generated parti-

2

cles with the detector and its response are implemented using the GEANT4 toolkit [24] as described in Ref. [25].

Signal $\overline{B}_s^0 \rightarrow D_s^- D_s^+$ candidates are reconstructed using four final states: (i) $D_s^+ \rightarrow K^+ K^- \pi^+$, $D_s^- \rightarrow K^- K^+ \pi^-$, (ii) $D_s^+ \rightarrow K^+ K^- \pi^+$, $D_s^- \rightarrow \pi^- \pi^+ \pi^-$, (iii) $D_s^+ \rightarrow K^+ K^- \pi^+$, $D_s^- \rightarrow K^- \pi^+ \pi^-$, and (iv) $D_s^+ \rightarrow \pi^+ \pi^- \pi^+$, $D_s^- \rightarrow \pi^- \pi^+ \pi^-$. In the normalization mode, $B^- \rightarrow D^0 D_s^-$, only the final state $D^0 \rightarrow K^- \pi^+$, $D_s^- \rightarrow K^- K^+ \pi^-$ is used. For the $\overline{B}_s^0 \rightarrow D^- D_s^+$ decay and the corresponding $B^0$ normalization mode, the $D^- \rightarrow K^+ \pi^- \pi^-$, $D_s^+ \rightarrow K^+ K^- \pi^+$ final state is used. Loose particle identification (PID) requirements are imposed on kaon and pion candidates, with efficiencies typically in excess of 95%. The $D$ candidates are required to have masses within $25\,\mathrm{MeV}/c^2$ of their known values [14] and to have vertex separation from the $B$ vertex satisfying $\chi^2_{\mathrm{VS}} > 2$. Here $\chi^2_{\mathrm{VS}}$ is the increase in $\chi^2$ of the parent $(B)$ vertex fit when the $(D$ meson$)$ decay products are constrained to come from the parent vertex, relative to the nominal fit. To suppress the large background from $\overline{B}_s^0 \rightarrow D_s^+ \pi^- \pi^+ \pi^-$ decays, $D_s^- \rightarrow \pi^- \pi^+ \pi^-$ candidates are required to have $\chi^2_{\mathrm{VS}} > 6$. As the signatures of $b$-hadron decays to double-charm final states are similar, vetoes are employed to suppress the cross-feed resulting from particle misidentification, following Ref. [26]. For the $D_s^+ \rightarrow K^+ \pi^- \pi^+$ decay, an additional veto to suppress cross-feed from $D^+ \rightarrow K^- \pi^+ \pi^+$ with double-misidentification is employed, which renders this background negligible. Potential background to $D_s^+$ decays from $D^{*+} \rightarrow D^0 \pi^+$ with $D^0 \rightarrow K^+ K^-$, $\pi^+ \pi^-$ is also removed by requiring the mass difference, $M(D^0 \pi^+) - M(D^0) > 150\,\mathrm{MeV}/c^2$. The production point of each $B$ candidate is taken as the PV with the smallest $\chi^2_{\mathrm{IP}}$ value. All $B$ candidates are refit taking both $D$ mass and vertex constraints into account [27].

The efficiencies of the PID and veto requirements are evaluated using dedicated $D^{*+} \rightarrow D^0 \pi^+$, $D^0 \rightarrow K^- \pi^+$ calibration samples collected at the same time as the data. The kinematic distributions of kaons and pions from the calibration sample are reweighted using simulation to match those of the $B$ decays under study. The combined PID and veto efficiencies are 91.4% for $B^- \rightarrow D^0 D_s^-$, 88.0% for $(\overline{B}_s^0, B^0) \rightarrow D^- D_s^+$, and 86.5%, 90.8%, 86.6%, and 95.9% for the $\overline{B}_s^0 \rightarrow D_s^- D_s^+$ final states (i)$-$(iv), respectively.

To further improve the signal-to-background ratio, a boosted decision tree (BDT) [28, 29] algorithm using seventeen input variables is employed. Five variables from the $B$ candidate are used, including $\chi^2_{\mathrm{IP}}$, the vertex fit $\chi^2_{\mathrm{vtx}}$ (with $D$ mass, and vertex constraints), the PV $\chi^2_{\mathrm{VS}}$, $p_{\mathrm{T}}$, and a $p_{\mathrm{T}}$ asymmetry variable [30]. For each $D$ daughter, $\chi^2_{\mathrm{IP}}$, the flight distance from the $B$ vertex normalized by its uncertainty, and the maximum distance between the trajectories of any pair of particles in the $D$ decay, are used. Lastly, for each $D$ candidate, the minimum $p_{\mathrm{T}}$, and both the smallest and largest $\chi^2_{\mathrm{IP}}$, among the $D$ daughter particles are used. The BDT uses simulated decays to emulate the signal and wrong-charge final states from data with masses larger than $5.2\,\mathrm{GeV}/c^2$ for the background. Here, wrong-charge refers to $D_s^\pm D_s^\pm$, $D^\pm D_s^\pm$, and $D^0 D_s^+$ combinations, where in the latter case we remove candidates within $30\,\mathrm{MeV}/c^2$ of the $B^+$ mass [14], to remove the small doubly-Cabibbo-suppressed decay contribution to this final state. The selection requirement on the BDT output is chosen to maximize the expected $\overline{B}_s^0 \rightarrow D_s^- D_s^+$ signal significance, corresponding to signal and background efficiencies of about 97% and 33%, respectively.
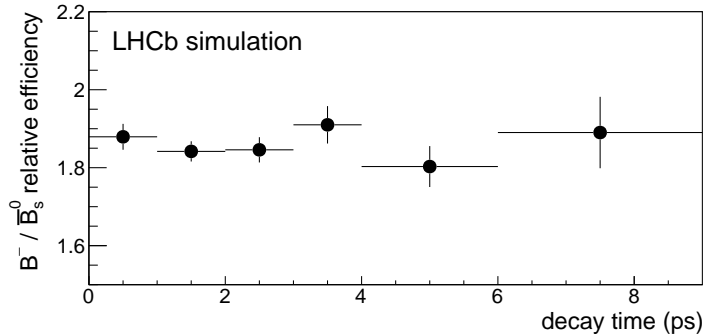
3

Figure 1: Ratio of selection efficiencies for $B^- \to D^0 D_s^-$ relative to $\overline{B}_s^0 \to D_s^- D_s^+$ decays as a function of decay time. The uncertainties shown are due to finite simulated sample sizes.

More than one candidate per event is allowed, but after all selections the fraction of events with multiple candidates is below 0.25% for all modes.

For the lifetime analysis, we consider only $B$ candidates with reconstructed decay time less than 9 ps. Signal efficiencies as functions of decay time are determined using simulated decays after all selections, except those that involve PID, as described above. The resulting $B^-$ to $\overline{B}_s^0$ relative efficiency as a function of decay time is shown in Fig. 1, where six decay time bins with widths ranging between 1 and 3 ps are used. For the $\overline{B}_s^0 \to D_s^- D_s^+$ decay, the efficiency used in the ratio is the weighted average of the $D_s^+ D_s^-$ final states (i)−(iv), where the weights are obtained from the observed yields in data. The efficiency accounts for the migration between bins, which is small since the resolution on the reconstructed time of ∼50 fs is much less than the bin width. Moreover, the time resolution is nearly identical for the signal and normalization modes, and is independent of the reconstructed lifetime. The relative efficiency is consistent with being independent of decay time, however, the computed bin-by-bin efficiencies are used to correct the data.

The mass distributions for the signal, summed over the four final states, and the normalization modes are shown in Fig. 2, along with the results of binned maximum likelihood fits. The $B$ signal shapes are each modeled using the sum of two Crystal Ball (CB) functions [31] with a common mean. The shape parameters are fixed from fits to simulated signal decays, with the exception of the resolution parameter, which is found to be about 15% larger in data than simulation. The shape of the low-mass background from partially reconstructed decays, where either a photon or pion is missing, is obtained from simulated decays, as are the cross-feed background shapes from $B^0 \to D^- D_s^+$ and $\Lambda_b^0 \to \Lambda_c^+ D_s^-$ decays ($\overline{B}_s^0 \to D_s^- D_s^+$ channel only). An additional peaking background due to $B \to DK^- K^+ \pi^-$ decays is also included in the fit. Its shape is obtained from simulation and the yield is fixed to be 1% of the signal yield from a fit to the $D$ mass sidebands. The combinatorial background shape is described by an exponential function with the shape parameter fixed to the value obtained from a fit to the mass spectrum of wrong-charge candidates. All yields, except that of the $B \to DK^- K^+ \pi^-$, are freely varied in the fit to the full data sample.
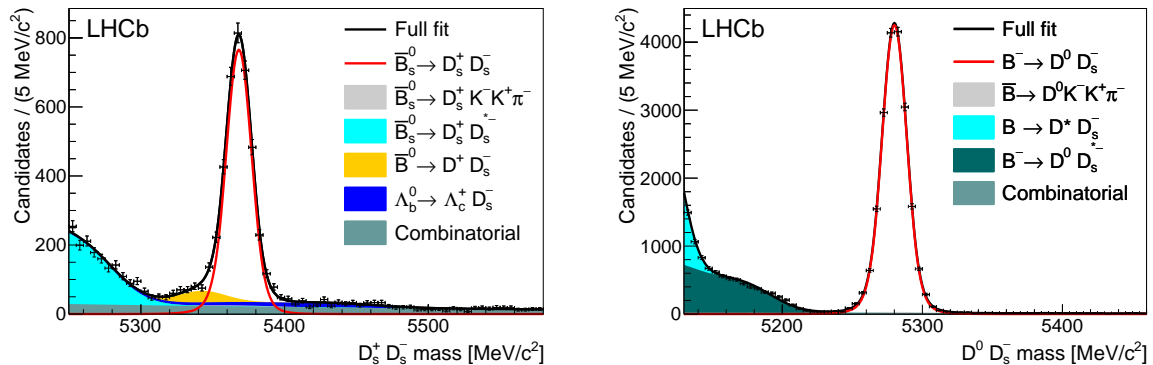
4

Figure 2: Mass distributions and fits to the full data sample for (left) $\overline{B}^0_s \to D^-_s D^+_s$ and (right) $B^- \to D^0 D^-_s$ candidates. The points are the data and the curves and shaded regions show the fit components.

In total, we observe $3499 \pm 65$ $\overline{B}^0_s \to D^-_s D^+_s$ and $19{,}432 \pm 140$ $B^- \to D^0 D^-_s$ decays. The data are split into the time bins shown in Fig. 1, and each mass distribution is fitted with the CB widths fixed to the values obtained from the full fit. The independence of the signal shape parameters on decay time is validated using simulated decays. The ratios of yields are then computed, and corrected by the relative efficiencies shown in Fig. 1. Figure 3 shows the efficiency-corrected yield ratios as a function of decay time. The data points are placed at the average time within each bin assuming an exponential form $e^{-t/(1.5\,\mathrm{ps})}$. Fitting an exponential function to the data yields the result $\alpha_{su} = 0.1156 \pm 0.0139 \,\mathrm{ps}^{-1}$. The uncertainty in the fitted slope due to using the value of 1.5 ps to get the average time in each bin is negligible. Using the known $B^-$ lifetime, $\tau^{\mathrm{eff}}_{\overline{B}^0_s \to D^-_s D^+_s}$ is determined to be $1.379 \pm 0.026\,(\mathrm{stat})$ ps.

As a cross-check, the full analysis is applied to the $B^- \to D^0 D^-_s$ and $B^0 \to D^- D^+_s$ decays, treating the former as the signal mode and the latter as the normalization mode. The fitted value for $\alpha \equiv 1/\tau_{B^0} - 1/\tau_{B^-}$ is $0.0500 \pm 0.0076 \,\mathrm{ps}^{-1}$, in excellent agreement with the expected value of $0.0489 \pm 0.0042$ [14]. This check indicates that the relative lifetime measurements are insensitive to small differences in the number of charged particles or lifetimes of the $D$ mesons in the final state. The $B^0 \to D^- D^+_s$ mode could have also been used as a normalization mode for the $\overline{B}^0_s \to D^-_s D^+_s$ time-dependent rate measurement, but due to limited simulated sample sizes it would have led to a larger systematic uncertainty.

As the method for determining $\tau^{\mathrm{eff}}_{\overline{B}^0_s \to D^-_s D^+_s}$ relies on ratios of yields and efficiencies, many systematic uncertainties cancel. The robustness of the relative acceptance is tested by subdividing the sample into mutually exclusive subsamples based on (i) center of mass energy, (ii) $D^-_s D^+_s$ final states, and (iii) hardware trigger decision, and searching for deviations larger than those expected from the finite sizes of the samples. The results from all checks were found to be within one standard deviation of the average. Based on the largest deviation, we assign a 0.010 ps systematic uncertainty due to the modeling of the relative acceptance. The statistical precision on the relative acceptance, as obtained from
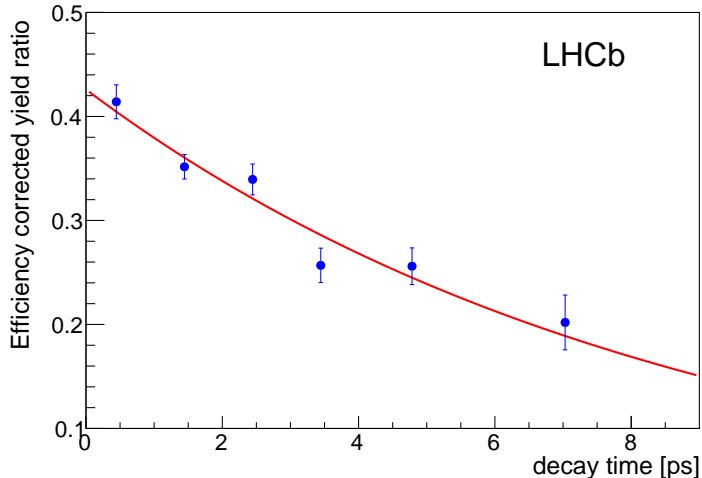
Figure 3: Efficiency corrected yield ratio of $\overline{B}_s^0 \to D_s^- D_s^+$ relative to $B^- \to D^0 D_s^-$ as a function of decay time, along with the exponential fit. The uncertainties are statistical only.

simulation, contributes an uncertainty of 0.011 ps. Using a different signal shape to fit the data leads to 0.003 ps uncertainty. If the combinatorial background shape parameter is allowed to freely vary in each time bin fit, we find a deviation of 0.001 ps from the nominal value of $\tau^{\mathrm{eff}}_{\overline{B}_s^0 \to D_s^- D_s^+}$, which is assigned as a systematic uncertainty. Due to the presence of a non-trivial acceptance function, the result of fitting a single exponential to the untagged $B_s^0$ decay time distribution does not coincide precisely with the formal definition of the effective lifetime [32]. The deviation between $\tau^{\mathrm{eff}}_{\overline{B}_s^0 \to D_s^- D_s^+}$ and the single exponential fit is at most 0.001 ps [32], which is assigned as a systematic uncertainty. The precision on the $B^-$ lifetime leads to 0.008 ps uncertainty on the value of $\tau^{\mathrm{eff}}_{\overline{B}_s^0 \to D_s^- D_s^+}$. Summing these deviations in quadrature, we obtain a total systematic uncertainty of 0.017 ps. In converting to a measurement of $\Gamma_{\mathrm{L}}$, an additional uncertainty due to a small $CP$-odd component of expected size $1 - \cos\phi_s = (0.1 \pm 3.2) \times 10^{-3}$ [5] leads to a bias no larger than $-0.001$ ps$^{-1}$. This is included in the $\Gamma_{\mathrm{L}}$ systematic uncertainty.

The value of $\tau^{\mathrm{eff}}_{\overline{B}_s^0 \to D_s^- D_s^+}$ and the corresponding decay width of the light $\overline{B}_s^0$ mass eigenstate are determined to be

$$\tau^{\mathrm{eff}}_{\overline{B}_s^0 \to D_s^- D_s^+} = 1.379 \pm 0.026 \pm 0.017 \text{ ps},$$
$$\Gamma_{\mathrm{L}} = 0.725 \pm 0.014 \pm 0.009 \text{ ps}^{-1},$$

where the first uncertainty is statistical and the second is systematic. These are the first such measurements using the $\overline{B}_s^0 \to D_s^- D_s^+$ decay. The measured effective lifetime represents the most precise measurement of the width of the light $\overline{B}_s^0$ mass eigenstate, and is about one standard deviation lower than the value obtained using $\overline{B}_s^0 \to K^+ K^-$ decays [8]. Compared to the $\overline{B}_s^0 \to D_s^- D_s^+$ decay, which is dominated by tree-level processes, the $\overline{B}_s^0 \to K^+ K^-$ decay is expected to have larger relative contributions from SM-loop
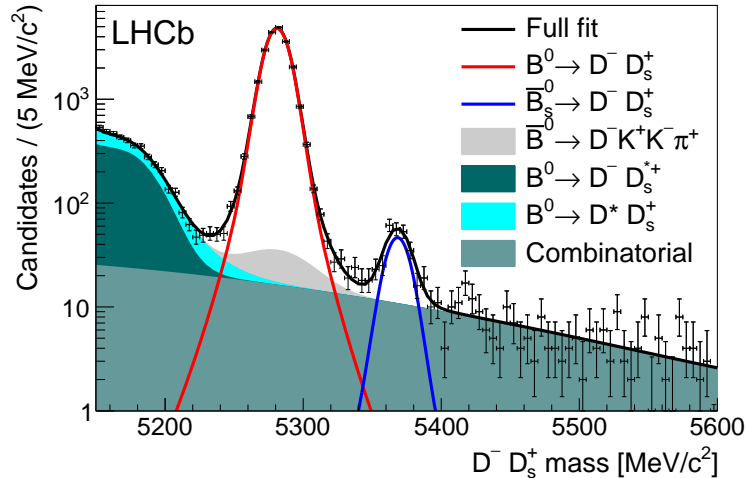
Figure 4: Mass distribution and fits to the full data sample for $\overline{B}_s^0$ and $B^0$ decays into the $D^- D_s^+$ final state. The points are the data and the curves and shaded regions show the fit components.

amplitudes [4, 33, 34], and therefore one should not naively average the effective lifetimes from these two decays. Moreover, if non-SM particles contribute additional amplitudes, their effect is likely to be larger in $\overline{B}_s^0 \to K^+ K^-$ than in $\overline{B}_s^0 \to D_s^- D_s^+$ decays [35].

The value of $\Gamma_{\rm L}$ obtained in this analysis may be compared to the value inferred from the time-dependent analyses of $J/\psi\, K^+ K^-$ and $J/\psi\, \pi^+ \pi^-$ decays. Using the values $\Gamma_s = 0.661 \pm 0.004 \pm 0.006$ ps$^{-1}$ and $\Delta\Gamma_s = 0.106 \pm 0.011 \pm 0.007$ ps$^{-1}$ [5], we find $\Gamma_{\rm L} = 0.714 \pm 0.010$ ps$^{-1}$, in good agreement with the value obtained from $\tau_{\overline{B}_s^0 \to D_s^- D_s^+}^{\rm eff}$.

The effective lifetime of the flavor-specific $\overline{B}_s^0 \to D^- D_s^+$ decay is also measured, using the $B^0 \to D^- D_s^+$ decay for normalization. The technique is identical to that described above, with the simplification that the relative efficiency equals one, since the final states are identical. Effects due to the mass difference between the $\overline{B}_s^0$ and $B^0$ mesons are negligible. A tighter BDT selection is imposed to optimize the expected signal-to-background ratio, which results in signal and background efficiencies of 87% and 11%, respectively. The mass spectrum and the corresponding fit are shown in Fig. 4, where the fitted components are analogous to those described previously. A total of $230 \pm 18$ $\overline{B}_s^0 \to D^- D_s^+$ and $21,195 \pm 147$ $B^0 \to D^- D_s^+$ decays are obtained. The time bins are the same as above, except the $6-9$ ps bin is dropped, since the yield in the signal mode beyond 6 ps is negligible. The relative decay rate is fitted to an exponential form $\mathcal{C}e^{-\beta t}$, where $\mathcal{C}$ is a normalization constant. The fitted value of $\beta$ is $0.000 \pm 0.068$ ps$^{-1}$. The systematic uncertainty due to the signal shape is 0.007 ps, obtained by using a different signal shape function. The exponential background shape is fixed in the nominal fit using $D^\pm D_s^\pm$ candidates, and a systematic uncertainty of 0.010 ps is determined by allowing its shape parameter to vary freely in the fit. In determining the effective lifetime, an uncertainty of 0.007 ps due to the limited precision of the $B^0$ lifetime [14] is also included. The resulting effective

7

lifetime in the $\overline{B}_s^0 \to D^- D_s^+$ mode is

$$\tau_{\overline{B}_s^0 \to D^- D_s^+}^{\mathrm{eff}} = 1.52 \pm 0.15 \pm 0.01 \text{ ps}.$$

This is the first measurement of the $\overline{B}_s^0$ lifetime using the $\overline{B}_s^0 \to D^- D_s^+$ decay. Its value is consistent with previous direct and indirect measurements of the $\overline{B}_s^0$ lifetime in other flavor-specific decays.

In summary, we report the first measurement of the $\overline{B}_s^0 \to D_s^- D_s^+$ effective lifetime and present the most precise direct measurement of the width of the light $B_s$ mass eigenstate. Their values are $\tau_{\overline{B}_s^0 \to D_s^- D_s^+}^{\mathrm{eff}} = 1.379 \pm 0.026 \pm 0.017$ ps and $\Gamma_{\mathrm{L}} = 0.725 \pm 0.014 \pm 0.009$ ps$^{-1}$. The $\Gamma_{\mathrm{L}}$ result is consistent with the value obtained from previously measured values of $\Delta\Gamma_s$ and $\Gamma_s$ [5]. We also determine the average $\overline{B}_s^0$ lifetime to be $1.52 \pm 0.15 \pm 0.01$ ps using the $\overline{B}_s^0 \to D^- D_s^+$ decay, which is consistent with other measurements.

# Acknowledgements

# References

[1] N. Cabibbo, *Unitary symmetry and leptonic decays*, Phys. Rev. Lett. **10** (1963) 531.

[2] M. Kobayashi and T. Maskawa, *CP violation in the renormalizable theory of weak interaction*, Prog. Theor. Phys. **49** (1973) 652.

[3] LHCb collaboration, R. Aaij *et al.*, *Precision measurement of the $B_s^0 - \overline{B}_s^0$ oscillation frequency $\Delta m_s$ in the decay $B_s^0 \to D_s^+ \pi^-$*, New J. Phys. **15** (2013) 053021, arXiv:1304.4741.

[4] R. Fleischer and R. Knegjens, *Effective lifetimes of $B_s$ decays and their constraints on the $B_s^0$-$\overline{B}_s^0$ mixing parameters*, Eur. Phys. J. **C71** (2011) 1789, arXiv:1109.5115.

[5] LHCb collaboration, R. Aaij *et al.*, *Measurement of CP-violation and the $B_s^0$-meson decay width difference with $B_s^0 \to J/\psi K^+ K^-$ and $B_s^0 \to J/\psi \pi^+ \pi^-$ decays*, Phys. Rev. **D87** (2013) 112010, arXiv:1304.2600.

[6] K. Hartkorn and H. Moser, *A new method of measuring $\Delta\Gamma/\Gamma$ in the $B_s^0$-$\overline{B}_s^0$ system*, Eur. Phys. J. **C8** (1999) 381.

[7] J. Charles *et al.*, *Predictions of selected flavour observables within the Standard Model*, Phys. Rev. **D84** (2011) 033005, arXiv:1106.4041.

[8] LHCb collaboration, R. Aaij *et al.*, *Measurement of the effective $B_s^0 \to K^+ K^-$ lifetime*, Phys. Lett. **B716** (2012) 393, arXiv:1207.5993.

[9] LHCb collaboration, R. Aaij *et al.*, *First measurement of time-dependent CP violation in $B_s^0 \to K^+ K^-$ decays*, arXiv:1308.1428, to appear in JHEP.

[10] LHCb collaboration, R. Aaij *et al.*, *Measurement of the $\overline{B}_s^0$ effective lifetime in the $J/\psi f_0(980)$ final state*, Phys. Rev. Lett. **109** (2012) 152002, arXiv:1207.0878.

[11] CDF collaboration, T. Aaltonen *et al.*, *Measurement of branching ratio and $B_s^0$ lifetime in the decay $B_s^0 \to J/\psi f_0(980)$ at CDF*, Phys. Rev. **D84** (2011) 052012, arXiv:1106.3682.

[12] LHCb collaboration, R. Aaij *et al.*, *Measurement of the $B_s^0 \to J/\psi K_S^0$ effective lifetime*, Nucl. Phys. **B873** (2013) 275, arXiv:1304.4500.

[13] R. Knegjens, *An exploration of $B_s \to J/\psi s\bar{s}$*, Nucl. Phys. **B241** (2013) 164, arXiv:1209.3206.

[14] Particle Data Group, J. Beringer *et al.*, *Review of particle physics*, Phys. Rev. **D86** (2012) 010001, and 2013 partial update for the 2014 edition.

[15] LHCb collaboration, A. A. Alves Jr. *et al.*, *The LHCb detector at the LHC*, JINST **3** (2008) S08005.

[16] M. Adinolfi *et al.*, *Performance of the LHCb RICH detector at the LHC*, Eur. Phys. J. **C73** (2013) 2431, arXiv:1211.6759.

[17] A. A. Alves Jr. *et al.*, *Performance of the LHCb muon system*, JINST **8** (2013) P02022, arXiv:1211.1346.

[18] R. Aaij *et al.*, *The LHCb trigger and its performance in 2011*, JINST **8** (2013) P04022, arXiv:1211.3055.

[19] V. V. Gligorov and M. Williams, *Efficient, reliable and fast high-level triggering using a bonsai boosted decision tree*, JINST **8** (2013) P02013, arXiv:1210.6861.

[20] T. Sjöstrand, S. Mrenna, and P. Skands, *PYTHIA 6.4 physics and manual*, JHEP **05** (2006) 026, arXiv:hep-ph/0603175; T. Sjöstrand, S. Mrenna, and P. Skands, *A brief introduction to PYTHIA 8.1*, Comput. Phys. Commun. **178** (2008) 852, arXiv:0710.3820.

[21] I. Belyaev *et al.*, *Handling of the generation of primary events in* GAUSS*, the LHCb simulation framework*, Nuclear Science Symposium Conference Record (NSS/MIC) **IEEE** (2010) 1155.

[22] D. J. Lange, *The EvtGen particle decay simulation package*, Nucl. Instrum. Meth. **A462** (2001) 152.

[23] P. Golonka and Z. Was, *PHOTOS Monte Carlo: a precision tool for QED corrections in Z and W decays*, Eur. Phys. J. **C45** (2006) 97, arXiv:hep-ph/0506026.

[24] Geant4 collaboration, J. Allison *et al.*, *Geant4 developments and applications*, IEEE Trans. Nucl. Sci. **53** (2006) 270; Geant4 collaboration, S. Agostinelli *et al.*, *Geant4: a simulation toolkit*, Nucl. Instrum. Meth. **A506** (2003) 250.

[25] M. Clemencic *et al.*, *The LHCb simulation application,* GAUSS*: design, evolution and experience*, J. Phys. Conf. Ser. **331** (2011) 032023.

[26] LHCb collaboration, R. Aaij *et al.*, *First observations of $\overline{B}_s^0 \to D^+D^-$, $D_s^+D^-$ and $D^0\overline{D}^0$ decays*, Phys. Rev. **D87** (2013) 092007, arXiv:1302.5854.

[27] W. D. Hulsbergen, *Decay chain fitting with a Kalman filter*, Nucl. Instrum. Meth. **A552** (2005) 566, arXiv:physics/0503191.

[28] L. Breiman, J. H. Friedman, R. A. Olshen, and C. J. Stone, *Classification and regression trees*, Wadsworth international group, Belmont, California, USA, 1984.

[29] R. E. Schapire and Y. Freund, *A decision-theoretic generalization of on-line learning and an application to boosting*, Jour. Comp. and Syst. Sc. **55** (1997) 119.

[30] LHCb collaboration, R. Aaij *et al.*, *Observation of the suppressed ADS modes $B^{\pm} \to [\pi^{\pm}K^{\mp}\pi^+\pi^-]_D K^{\pm}$ and $B^{\pm} \to [\pi^{\pm}K^{\mp}\pi^+\pi^-]_D \pi^{\pm}$*, Phys. Lett. **B723** (2013) 44, arXiv:1303.4646.

[31] T. Skwarnicki, *A study of the radiative cascade transitions between the Upsilon-prime and Upsilon resonances*, PhD thesis, Institute of Nuclear Physics, Krakow, 1986, DESY-F31-86-02.

[32] K. De Bruyn *et al.*, *Branching ratio measurements of $B_s$ decays*, Phys. Rev. **D86** (2012) 014027, arXiv:1204.1735.

[33] R. Fleischer, *New strategies to extract $\beta$ and $\gamma$ from $B_d \to \pi^+\pi^-$ and $B_s \to K^+K^-$*, Phys. Lett. **B459** (1999) 306, arXiv:hep-ph/9903456.

[34] R. Fleischer, *Exploring CP violation and penguin effects through $B_d^0 \rightarrow D^+ D^-$ and $B_s^0 \rightarrow D_s^+ D_s^-$*, Eur. Phys. J. **C51** (2007) 849, arXiv:0705.4421.

[35] R. Fleischer and R. Knegjens, *In pursuit of new physics with $B_s^0 \rightarrow K^+ K^-$*, Eur. Phys. J. **C71** (2011) 1532, arXiv:1011.1096.